LAWRENCE
LIVERMORE
NATIONAL
LABORATORY

LLNL-JRNL-564832

Final compression beamline systems for heavy ion fusion drivers

Y. Y. Lau, S. S. Yu, J. J. Barnard, P. A. Seidl

July 17, 2012

Laser and Particle Beams

Disclaimer

Final compression beamline systems for heavy ion fusion drivers

Y. Y. Lau (a), Simon S. Yu (a)(b), John J. Barnard (c) and Peter A. Seidl (b)
(a) The Chinese University of Hong Kong, Shatin, Hong Kong
(b) Lawrence Berkeley National Laboratory, Berkeley, California, USA
(c) Lawrence Livermore National Laboratory, Livermore, California, USA

Abstract

We have identified a general final compression section for HIF drivers, the section between accelerator and the target. The beam are given a head to tail velocity tilt at the beginning of the section for longitudinal compression, while going through bends which direct it to the target at specific angle. The aim is to get the beams compressed while maintaining a small centroid offset after the bends. We used a specific example 1MJ driver with 500MeV Rb+1 ion beams. We studied the effect of minimizing dispersion using different bend strategies, and came up with a beamline point design with adiabatic bends. We also identified some factors that lead to emittance growth as well as the minimum pulse length and spot size on the target.

1. INTRODUCTION

In current designs of heavy ion fusion drivers, manipulating multiple intense heavy ion beams is usually involved. For both direct and indirect drive, a drift compression section [1-3] is needed between the accelerators and the fusion chamber, to direct the beams towards the target at specific geometry and compress them at the same time for the short pulse lengths required for target ignition. It is shown that a simple 4-polar-rings beam configuration around the target can achieve high uniformities with rotated beams. [4] The benefit of this configuration can be maximized if the polar axis is aligned with the accelerators on both sides, then only 2 designs of channels will be needed as the polar symmetry implies they will be nearly identical within the same group (Fig. 1). In general, the number of channel and target angles can vary depending on need, so the configuration works for any multiple beam direct or indirect drivers. We take the 1 MJ direct driver with 500 MeV Rb+1 beams as an example.

Each beam channel consists of bends, a matching section and a neutralized drift section. The beam is confined by a FODO lattice of quadrupole magnets, which also combines the function of bending dipoles. We use a constant focusing strength in this study, so as the beam compresses longitudinally, it expands transversely. There are two sets of bends in opposite directions (+x and –x), turning the beam by a total roughly 37 degree, which corresponds to one of the polar angle in the 4-ring configuration. The beam then goes through the last four quads, which match the beam envelope to circular shape, into a plasma-filled neutralized drift section. [1] It will get compressed down to the final length by the residual velocity tilt. A strong solenoid is placed at several meters away from the target for final focusing.

We used the 3D particle-in-cell code WARP [5] to simulate the beam in this study. The semi-Gaussian beam starts with a parabolic current profile and a matched envelope. The amount of initial velocity tilt, peak current and pulse length are variable within ranges of the typical values. Table 1 shows some parameters used in this study. Due to a relativity high beam perveance, a high velocity tilt is desirable for overcoming the space charge force and compressing the beam quickly. We choose a 10% tilt and a short drift length of roughly 100 m.

Table 1 Parameters used in this study

Parameter	Value
Initial peak current/beam (A)	100.0
Energy/beam (kJ)	7.5
Initial perveance	5.35×10^{-5}
Initial pulse length, r.m.s. (ns)	51
Initial transverse emittance (π m rad)	5.2×10^{-5}
Initial longitudinal emittance (π m rad)	4.56×10^{-3}
Velocity tilt	-10%
Section total length (m)	≈91
Bend length (m)	20, 30
Neutralized drift length (m)	≈27
Lattice period (m)	2.0
Quad length (m)	0.8
Quad strength (T/m)	64.33
Max dipole strength (T)	4.65
Undepressed tune (degree)	72
Pipe radius (cm)	10

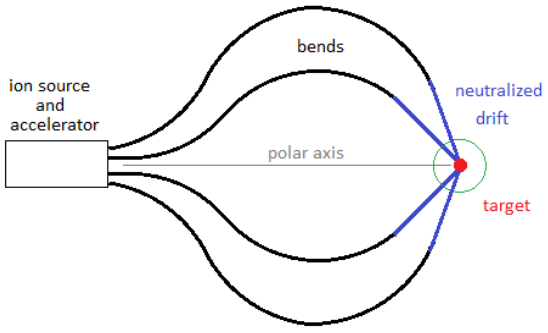

Fig. 1 Overview of beam channels geometry. The opposite side (which is not shown here) is identical.

2. BEND STRATEGIES

As a result of the high velocity tilt, beam slices with different momentum travel orbits with various curvatures, which leads to beam dispersion. The short drift length will leads to sharper bends which impose further difficulties. In designing the bends, we take the idea in a previous paper, which showed that the centroid offset can be kept at minimum by varying bend strength [2]. We adopted similar bend strategies, namely abrupt bend, matched bend and adiabatic bend. However, due to the limited drift length, for the adiabatic bend, instead of varying bend strength slowly over several (undepressed) betatron periods, we used a linear ramp of 1 betatron period for both up and down. Also all the bend lengths are integral multiples of the betatron period for the best achromaticity. The dipole strength of each strategy is shown as follow.

Table 2 Dipole strength associated with each bend strategy

Design	First arc values (T)	Second arc values (T)
Abrupt bend	2.38	2.38
Matched bend	1.69, 3.38	1.49, 2.98
Adiabatic bend	Max 4.65	Max 3.57

Fig. 3 shows the evolution of centroid offset for an off-momentum slice of the beam. The maximum offsets of the beam tips at end of the bend (z = 55.5 m) are 3.4 mm, 1.3 mm and 0.8 mm respectively for the three bend cases. It is clear that an adiabatic or a matched design result in significant lower offset then an abrupt design. The drawback is they require stronger dipole field.

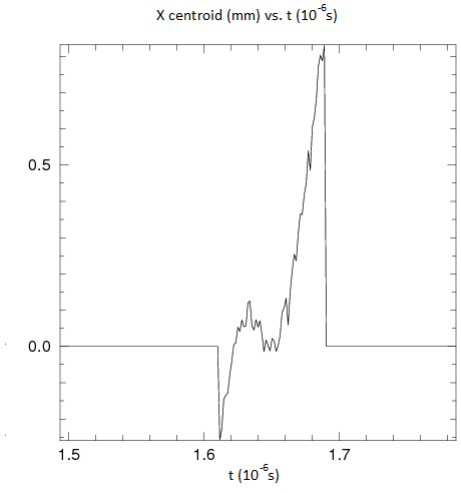

Fig. 2 Beam centroid of the whole beam as a function of t at bend end (z = 55.5 m) for adiabatic case. The maximum offset here is about 0.8 mm.

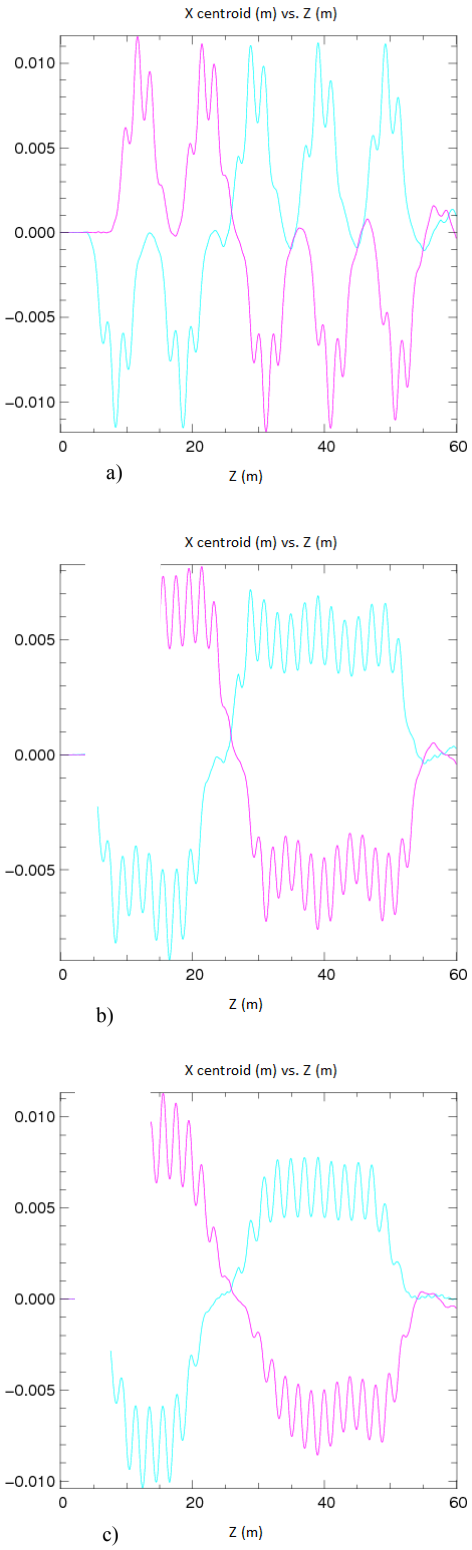

Fig. 3 Beam centroid as a function of z for the case: a) abrupt bend, b) matched bend and c) adiabatic bend, for two slices halfway to the beam head and tail respectively.

3. NEUTRALIZED DRIFT SECTION AND FINAL FOCUS

The straight section after the bends is the neutralized drift section, in which the space charge force is assumed to be completely gone in the simulations. It starts at z = 64.6 m and there is roughly 27 m away from the longitudinal focus for an approximately 6.5% residual tilt. Within this region the beam is allowed to expand transversely by a slight angle generated by the matching quads, this is desirable for the final spot size. With a 12 T solenoid at 4 m away, we get a 5 mm spot, 0.08 m (2.4 ns) pulse length at z = 91 m (Fig. 4 and Fig. 5).

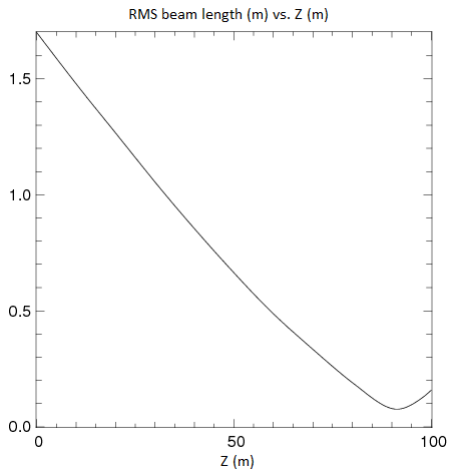

Fig. 4 Beam length as a function of z.

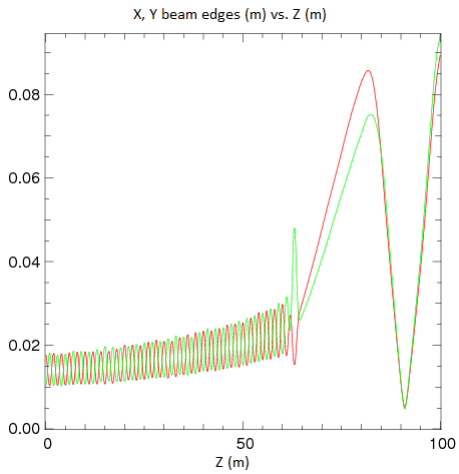

Fig. 5 Beam edges as function of z, red line is x and green line is y respectively.

As a result of no space charge, the final spot and pulse length will depend mainly on the emittances in the corresponding directions. To look at this effect, we repeat the simulations with reduced initial emittances in both directions. Which are 1/2, 1/4 of the first run values, and lastly with zero emittances. Emittances in the two directions are defined respectively as:

$$\varepsilon x = 4\sqrt{\Delta x^2\,\Delta x'^2 - \Delta x\,\Delta x'^2} \quad (1)$$

$$\varepsilon z = 4\sqrt{v_z\Delta z^2\,\Delta v_z^2 - \Delta z\,\Delta v_z^2} \quad (2)$$

where $\Delta x = x - \bar{x}$ and all similar quantities are the derivation from the mean and $\bar{}$ denotes average over particles.

Table 3 Spot sizes with different initial εx values

Initial ($10^{-5}\pi$ m rad)	Spot size (mm)	Central slice spot(mm)
5.2	5.6	5.2
2.6	4.2	4.0
1.3	3.0	2.8
0.0	2.6	2.1

Table 4 Final pulse length and final peak current with different initial εz, note that the longitudinal focus occurs at slightly further away with lower εz

Initial ($10^{-3}\pi$ m rad)	Final rms length (ns)	Final current (A)
4.56	2.26	2050
2.28	1.34	3900
1.14	0.83	7000
0.00	0.60	12200

Table 3 and Table 4 show the results with different initial emittances. The final pulse length and current are typical requirement values for HIF drivers. However, we did not get a small spot even with the smallest possible transverse emittance and a reasonable maximum final converging angle, limited by the pipe radius, solenoid strength and size of the fusion chamber. The spot size is partly due to chromatic effect, as a result of the residual velocity tilt, the beam head and tail have different focal lengths (Fig. 6). It is clear that even in this case the spot is dominated by emittance.

We take the case with small initial values (Case 3 in the above) as an example to illustrate the fundamental emittance limit. Fig. 7 shows ε_x ,ε_y and ε_z vs. z, we observe the following: (1) εz grows steadily with the distance travelled in vacuum section but remains constant in neutralized section, so it is believed that εz growth is only due to space charge force. (2) ε_x is affected by the bends as there are clear rises at the locations. (3) ε_x and ε_y tends to equilibrate as seen from the region before the neutralization, still ε_x ends up larger than ε_y. The value at the focus is about 3×10^{-5} π m rad. More detailed analysis on factors affecting emittance growth will be made in future works.

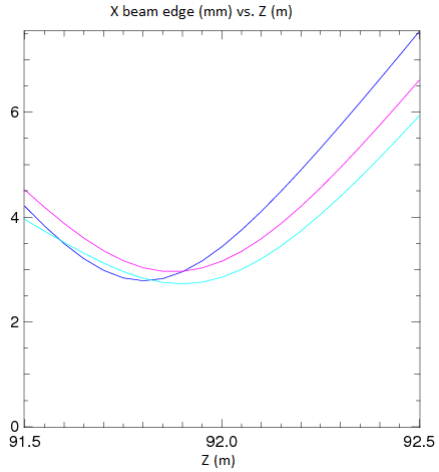

Fig. 6 Beam edge as function of z near the focus for the case with low initial emittances, blue line corresponds to central slice; purple and cyan lines are off momentum slices near the beam tail and head respectively.

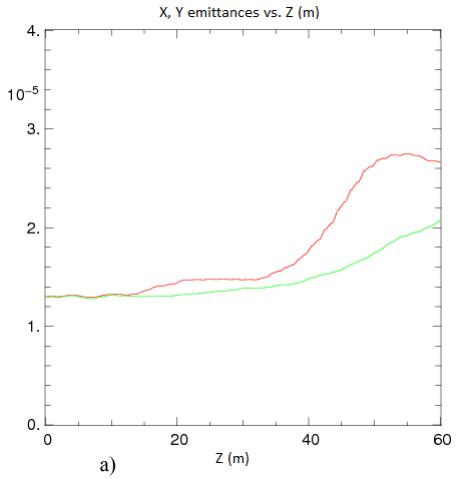

a)

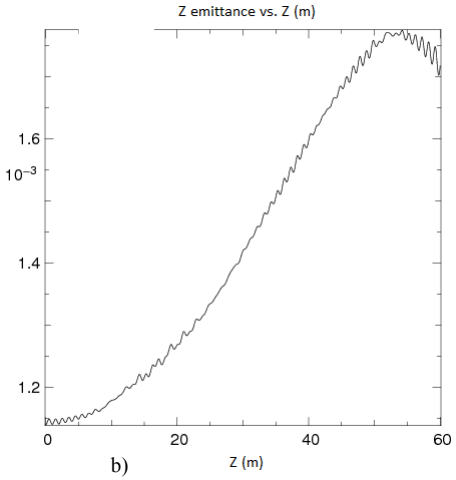

b)

Fig. 7 a) ε_x (red line) and ε_y (green line) of beam central slice vs. z b) ε_z of the whole beam vs. z.

4. CONCLUSIONS

We have proposed here a general strategy to layout the final compression beamline for any multiple beam direct and indirect drivers, which utilizes the symmetry to simplify the design of individual beam channels. We have also shown some key features using an example of a relatively low energy, high perveance beam with parameters compatible with a full driver system. The adiabatic bend design used in this study works well, even with a relativity high velocity tilt and short drift length.

We observed emittance growth in the section which will place constraints on the final spot size and pulse length on the target. Particularly in the example studied, more advanced and carefully designed focusing schemes may be necessary to compress the spot sizes to meet target requirements. Some mechanisms for emittance growth and the parametric dependence are being investigated; the results will be published elsewhere.

ACKNOWLEDGMENTS

Work performed by one of the authors (JJB) under the auspices of the U.S. Department of Energy under contract DE-AC52-07NA27344 at LLNL, and by one of the authors (PAS) under University of California contract DE-AC02-05CH11231 at LBNL.

REFERENCES

[1]P. K. Roy *et al.* (2005); Drift Compression of an Intense Neutralized Ion Beam. *Phys. Rev. Lett.* **95**, 234801

[2] E. P. Lee and J. J. Barnard (2002); Bends and Momentum Dispersion during Final Compression in Heavy Ion Fusion Drivers. *Laser and Particle Beams* **20**, 581

[3] De Hoon, M. J. L. (2001); *Drift Compression and Final Focus Systems for Heavy Ion Inertial Fusion*, Ph.D. Thesis, University of California, Berkeley.

[4] J. Runge and B. G. Logan (2009); Nonuniformity for rotated beam illumination in directly driven heavy-ion fusion. *Physics of Plasmas* **16**, 033109

[5] D. P. Grote *et al.* (2005); The WARP Code: Modeling High Intensity Ion Beams. *AIP Conf. Proc.* **749**, 55